Agricultural and Forest Meteorology 242 (2017) 75–84

Contents lists available at ScienceDirect

Agricultural and Forest Meteorology

journal homepage: www.elsevier.com/locate/agrformet

Research paper

Experimental validation of footprint models for eddy covariance CO_2 flux measurements above grassland by means of natural and artificial tracers

Nicola Arriga[a,b,*], Üllar Rannik[c], Marc Aubinet[d], Arnaud Carrara[e], Timo Vesala[c,f], Dario Papale[a,g]

[a] Department for Innovation in Biological, Agro-food and Forest Systems (DIBAF), University of Tuscia, Viterbo, Italy
[b] Research Centre of Excellence Plants and Ecosystems (PLECO), University of Antwerp, Wilrijk, Belgium
[c] Department of Physics, University of Helsinki, Helsinki, Finland
[d] University of Liege, Gembloux Agro-Bio Tech, TERRA Research Centre, Gembloux, Belgium
[e] CEAM, Fundación de la Comunidad Valenciana Centro de Estudios Ambientales del Mediterraneo, Paterna, Spain
[f] Department of Forest Sciences, University of Helsinki, Helsinki, Finland
[g] Euro-Mediterranean Center on Climate Change (CMCC), Lecce, Italy

ARTICLE INFO

Keywords:
Lagrangian footprint simulations
Eddy covariance
Manipulation experiments
Surface roughness

ABSTRACT

Footprint models, which simulate source area for scalar fluxes, are fundamental tools for a correct interpretation of micromoeteorological flux measurements and ecosystem exchange inferred from such data. Over the last two decades models of varying complexity have been developed, but all of them suffer from a significant lack of experimental validation. In this study two different experimental tests have been conducted with the aim of offering validation: a manipulation of the vegetation cover and an artificial tracer emission. In the first case the extension of the flux source has been changed progressively by successive cuts of vegetation, while in the second case by varying the distance of a tracer emission line respect to the measurement point. Results have been used to validate two analytical and a numerical footprint models. The experimental data show a good agreement with footprint models and indicate a limited extension of the flux source area, with approximately 75% of the sources confined within a range of 10–20 times the effective measurement height, i.e. the measurement height above the zero plane displacement. Another interesting result was the strong dependence on the surface roughness of both experimental estimates and numerical simulations of footprint. The effect of surface roughness on experimental results and models outputs was comparable to the effect of atmospheric stability. This indicates that surface roughness and turbulence conditions may play a significant role in source area location, in particular above inhomogeneous surfaces with change in roughness, as in the case of the manipulation experiment. Consequently a careful site specific quantification of these parameters seems to be fundamental to obtain realistic footprint estimates and significantly improve eddy covariance flux interpretation at complex sites.

1. Introduction

The eddy covariance (EC) methodology allows the quantification of mass and energy exchanges between earth surfaces and atmosphere by measurements of wind speed, air temperature and passive tracer concentrations at time scales enabling the capture of a wide range of turbulent motions (Aubinet et al., 1999). The fluxes between ecosystem and atmosphere measured by the EC methodology are originated from an area surrounding, mostly upwind, the measurement point: the source area. The mathematical relation between the spatial distribution of the flux sources and the corresponding magnitude is termed footprint function or source weight function (Horst and Weil, 1992; Leclerc and Thurtell, 1990; Schmid, 1994; Schmid, 2002) Frequently the evaluation of source area for EC measurements is also referred to as the footprint analysis and both terms are interchangeable (Vesala et al., 2008). The estimation of the source area associated with each single flux measurement is important information that facilitates data interpretation and quality filtering (Göckede et al., 2004; Nicolini et al., 2015; Rebmann et al., 2005). It is of primary importance for analysis integrating both EC and remote sensing data, but also for interpretation of EC data collected in ecosystems that are heterogeneous in terms of land use, vegetation, biophysical characteristics such as leaf area index, biomass, soil type and management. The dimensions of the effective source area are influenced by structural properties of the surface (e.g. roughness), by the measurement height and by micrometeorological conditions (e.g. wind speed and direction, turbulence intensity, atmospheric stability). A footprint function model describes how the factors above influence the spatial distribution of the flux sources. Four categories of

* Corresponding author at: Research Centre of Excellence Plants and Ecosystems (PLECO), Biology Department, University of Antwerp, Universiteitsplein 1B, 2610 Wilrijk, Belgium.
E-mail address: Nicola.Arriga@uantwerpen.be (N. Arriga).

http://dx.doi.org/10.1016/j.agrformet.2017.04.006
Received 29 August 2016; Received in revised form 7 April 2017; Accepted 17 April 2017

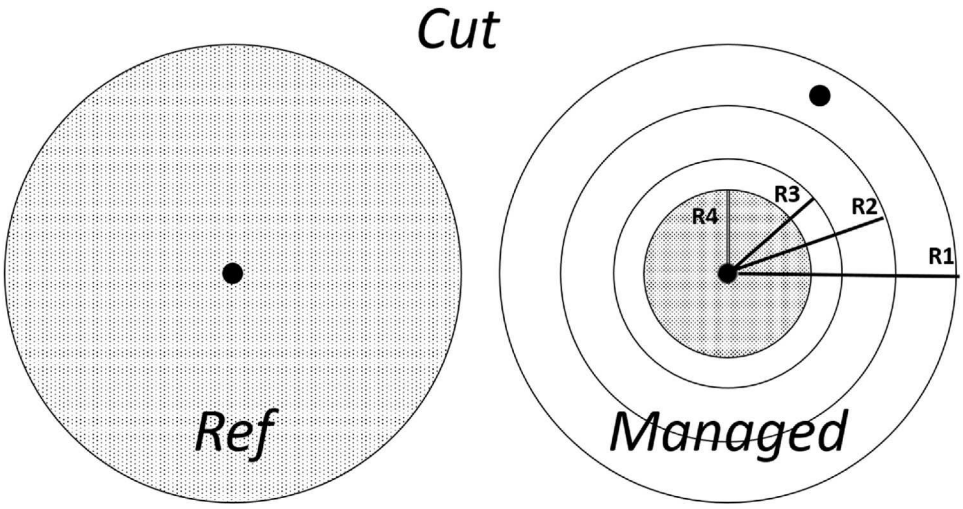

Fig. 1. Sketch of the ME experiment with Ref oats disc on the left and Managed disc on the right. Dots represent the position of the three EC systems. R1 to R4 are the radii of the successive oats cover after each cut in the Managed plot, respectively 30 m, 22 m, 15 m and 11 m.

models of different theoretical and practical complexity have been proposed in the last two decades (Leclerc and Foken, 2014; Rannik et al., 2012): (1) analytical models, (2) Lagrangian stochastic particle dispersion models, (3) large-eddy simulation and (4) ensemble-averaged closure models. As pointed out in past studies (Foken and Leclerc, 2004; Vesala et al., 2008) experimental footprint analyses and simulations are rare, in particular due to the complexity of the technical set-up and to the related costs. Nevertheless a number of experiments have been specifically designed, realized and published. Some authors (Finn et al., 1996; Leclerc et al., 2003) used an artificial emission of tracer gas, SF_6, to validate footprint models, while others (Aubinet et al., 2001; Göckede et al., 2004; Göckede et al., 2005; Marcolla and Cescatti, 2005; Neftel et al., 2008) used spatial heterogeneity of the surface composition for the same scope with different footprint models, mainly analytical. However the experimental validation of the footprint models and the uncertainty in source area evaluation is still a major issue for flux data interpretation. Reducing uncertainties in the estimation of the source area extension would also lead to the development of more accurate footprint models and to pinpointing the optimal location for an EC site. This information would be particularly important to measure fluxes over small vegetation patches, for example in the case of ecosystem manipulation experiments in which ecological or meteorological driving forces such as, e.g., temperature, water or nutrients availability, are modified over grassland and cropland fields generally not larger than few hundred square meters.

In this study two different field experiments have been conducted where the source area has been manipulated with the aim of measuring the effective footprint extension. In the first experiment the surface has been modified altering the vegetation cover while in the second an artificial CO_2 source has been used as a tracer. In both cases the results have been compared with the output of analytical and Lagrangian footprint models. Specifically, the objectives of this paper are: (1) to assess the effect of manipulation of the scalar sources on EC flux measurements and (2) to compare the results of various kind of footprint models with experimental data.

2. Materials and methods

The experimental site was located in Viterbo, Italy, in the area of the University of Tuscia Didactical Farm (42°25′16.10″N, 12°04′37.26″E). The selected area was a flat agricultural field approximately 130 × 95 m in size. This area was planted with oats (Avena sativa L.) at the end of 2007 and the measurements were taken between April and October 2008. The following two experiments were conducted:

- A manipulation experiment (ME) by means of successive cuts of the vegetation cover in the source area to modify its surface extension and to see the effect on the measured flux compared to a reference plot.
- A controlled emission of CO_2 as an artificial tracer (AT) with the aim of estimating the dependence of the footprint function from the distance of the emitting point.

Vegetation species shorter than oats were initially taken into consideration for the ME in order to limit the impact of the roughness step change between cut and uncut areas covered by oats and the consequent formation of internal boundary layer (IBL) (Garratt, 1992). However the footprint management in order to get a clear difference between harvested and not-harvested areas would have been more difficult and uncertain with short vegetation and for this reason this option was excluded. Details of each experiment are described in the following subsections 2.1 and 2.2.

2.1. Source area manipulation experiment (ME)

The first experimental footprint test has been realized with an artificial manipulation of the surface distribution of carbon dioxide sources and sinks in proximity of the EC instrumentation. The covering of oats was cut in order to only keep two discs of intact vegetation of equal dimension, approximately 30 m of radius (Ref and Managed, see Fig. 1). The mean canopy height (h_c), measured before the beginning of the manipulation in 30 points randomly distributed, was h_c = 1.02m. This experiment took place since day of the year (doy) 132–163 of 2008.

An EC system equipped with a sonic anemometer (model Gill-R3, Gill Instruments Ltd, Lymington, Hampshire, UK) and an infra-red gas analyzer (model LI-7500, LI-COR Inc., Lincoln, NE, USA) was placed in the center of Managed disc at 2.35 m above the soil and a second Gill R3 sonic anemometer was placed at 1.4 m. Another identical EC system was placed in the center of the Ref disc at the same height. A third EC system of the same type of the other two was placed from doy 151 to doy 162 above the Cut surface at a height of 1.5 m to measure the contribution of the external mowed crowns to the flux measured in the center of the Managed plot. This measurement height was selected to minimize the source area of the cut plot. Lateral separation between sonics and analyzers was 20 cm, while analyzers were always placed 5 cm below the sonics to minimize spectral loss due to the short distance of the canopy top. In accordance with other studies (Horst and Lenschow, 2009; Kristensen et al., 1997) we did not expect such a small

Table 1
Radius of the oats covered disc in the Managed and Ref plot during successive periods.

	DOY: 132–139	DOY: 139–149	DOY: 149–155	DOY: 155–163
Managed	30m	22m	15m	11m
Ref	30m	30m	30m	30m

vertical separation to influence significantly the measuring procedure. All the LI-7500 gas analyzers were tilted by 30° in relation to the vertical direction and pointed towards the North to minimize effect of direct solar radiation. Data were continuously sampled at 20 Hz. The raw data were processed using eco2s EC software (available at http://gaia.agraria.unitus.it/eco2s): time lag optimization through covariance maximization, linear detrending and 2D rotation were selected among the possible processing options (Rebmann et al., 2012). Fluxes were corrected accounting for Webb-Pearman-Leuning (WPL) term (Webb et al., 1980), spectral loss due to sonic path length, spatial separation and limited response time following low-pass filtering spectral correction procedure proposed by Moncrieff et al. (1997). A first set of parallel measurements was recorded with the same vegetation extension in Managed and Ref plots. Following this the vegetation in the Managed plot was periodically cut in the external circumference to otain a progressive reduction of its radius and, consequently, of the source area covered by vegetation with the time schedule reported in Table 1. The Ref disc was kept with the original radius throughout the whole experiment and used as a reference. Cut vegetation in the Managed disc was immediately removed. The contribution (α) of the progressively reduced source area to the carbon flux in the Managed plot ($Fc_{Managed}$) has been evaluated with the following formula:

$$Fc_{Managed} = \alpha Fc_{Ref} + (1 - \alpha)Fc_{Cut} \quad (1)$$

where Fc_{Ref} is the carbon flux measured by the Ref system at 2.35m, while Fc_{Cut} is the carbon flux emitted from the cut surface, estimated fitting an ecosystem respiration model to the measurements of carbon fluxes and air temperature (Reichstein et al., 2005). The wind direction analysis, see wind rose in Fig. 2, showed two dominant wind directions in the study period, i.e. South-SouthWest and North-NorthEast, with very limited contributions from other sectors. To exclude possible disturbances from unavoidable upwind obstacles at the site, the following angular sectors for wind directions were excluded: a) 30° < θ < 60°; b) 120° < θ < 160°; c) 270° < θ < 360°. The

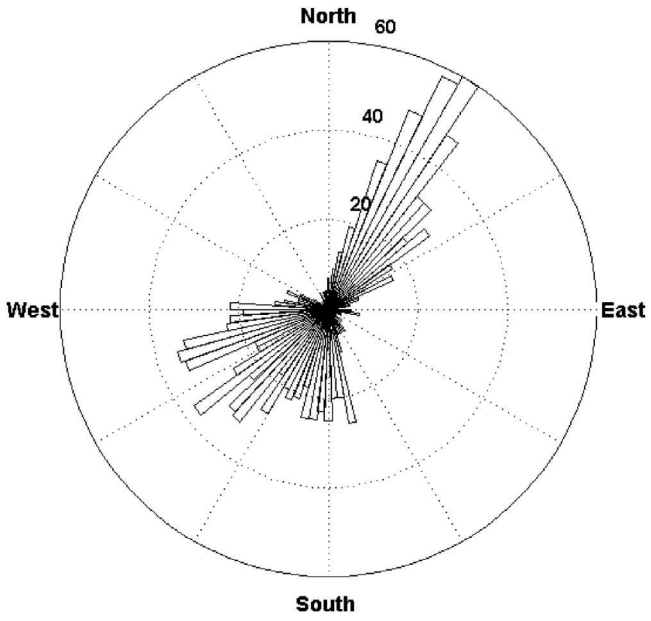

Fig. 2. Wind rose from the ME database.

assumption under Eq (1) was that a percentage α of the flux originated from the uncut internal circle having the same flux as the Ref plot and the remaining contribution (1-α) was due to the emission from the cut external crown in the surface of the Managed plot that was no longer covered by oats. This parameter is equivalent to the cumulative footprint obtained by along-wind integration of the modelled footprint density function from the measurement point to the limit of the vegetation. The underlying hypothesis was that the initial plots of the same vegetation cover included the entire source area of the respective EC systems under the conditions considered in the analysis. The Ref measurement height was 2.35 m above a dense canopy of 1.0m. In these conditions a radius of 30 m corresponds to approximately twenty times the effective measurement height (h_{eff}) calculated with respect to zero plane displacement d ($h_{eff} = z_m - d$), where z_m is the measurement height relative to the soil surface. The parameter d was estimated to be d = 0.91 m by means of vertical profile of turbulence statistics collected above the Ref plot using four sonic anemometers (data not shown). Such distance to measurement height ratio, according to published footprint analysis (Leclerc and Foken, 2014; Leclerc et al., 2003), includes most part of the sources and sinks for an EC flux in the roughness sublayer and justifies the assumption that the entire source area was included in the oats discs with 30 m radii. Moreover the value of the parameter α calculated for the initial period when both circles had the same radius is close to one as it was theoretically expected for measurements collected above surfaces with the same vegetation. Flux data used to calculate α were selected by removing the outliers, i.e. values outside the range [− 50 $\mu molm^{-2}s^{-1}$; + 50 $\mu molm^{-2}s^{-1}$]. Values of the stability parameter (z − d)/L, where L is the Monin-Obukhov length, were derived from measurements collected by sonic anemometer of the EC system in the Ref plot, i.e. 2.35 m above the soil. Stable stratification conditions were excluded from the analysis because in such situations source areas are expected to extend for longer distances (Vesala et al., 2008). Moreover, footprint models are generally not well defined for these particular atmospheric conditions and EC methodology requirements are frequently challenged by low intensity of turbulence and a high degree of non-stationarity.

2.2. Artificial tracer experiment (AT)

The second experiment of footprint evaluation has been realized with artificial tracer emission. The field was completely cut after the manipulation experiment leaving just very short grass residuals without photosynthetic activity. A system for release of gaseous CO_2 was constructed and placed at various distances upwind of the EC systems (see the scheme in Fig. 3). The release system was done using a 40 m long tube of plastic material (PTFE) with an internal and external diameter of 6 mm and 8 mm, respectively. Eight release ports were equally spaced along this line. In each port a manual flow regulator was installed and the tube was connected to a rack with six tanks of compressed CO_2. The outflow was regulated by a pressure regulator and monitored by another manual flow regulator to keep flow rate at a set-point of 80 slpm. A portable manual flow meter was used to check CO_2 emission from single ports during the experiment to ensure constant outflow from each port along the release line. A fixed vertical profile of three identical EC systems was installed downwind at measurement heights from the soil of 0.7 m, 1.7 m and 2.3 m. A fourth EC system was installed 75 m upwind from the vertical profile at 2.3 m from the soil, as a reference to measure the background flux of CO_2. All four EC systems were composed of a Gill R3 sonic anemometer and a LI-7500 gas analyzer. The release line has been placed orthogonally to the main wind direction at six different distances from the EC profile: 38 m, 23.2 m, 13.6 m, 9.5 m, 5.5 m upwind from the measurement mast and 4.5 m downwind. The relative position of the release line and measuring systems was decided upon based on the prevailing wind direction occurring during the experiment. This set-up aimed to simulate a strong CO_2 linear emission distributed orthogonally to the wind direction (i.e.

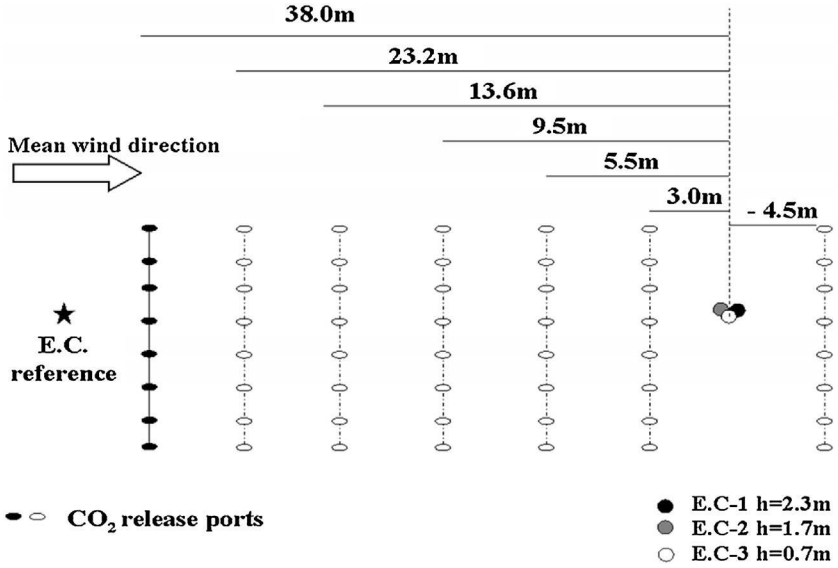

Fig. 3. Sketch of the AT experiment with positions of the release line respect to vertical profiles of EC systems (right) and reference EC system (left).

crosswind) and to quantify the effect of such emissions on EC systems placed at different heights downwind and upwind. In this way it was possible to obtain an experimental crosswind integrated footprint function curve for each measurement height by the ratio between the measured flux (F_c) and the linear source emission strength (Q), i.e. the emitted quantity of CO_2 per unit length in the unit of time. Raw EC data were processed following the same procedures described in Section 2.2. Dependence of crosswind speed variance on height has been analyzed at the three measurement levels to see if the variable affecting lateral dispersion varied significantly with height. The ratio $\sigma(v)/u_*$, where $\sigma(v)$ is the standard deviation of crosswind speed component, has been evaluated for all measurement levels and its relative deviation at 0.7 m and 1.7 m compared to the value at 2.3 m has been found to be, on average, 14.5%, thus with limited variability between the three measurement levels.

2.3. Footprint function modeling

The experimental data collected in the ME and AT experiments were compared with the results of two analytical footprint models, the Schuepp model (Schuepp et al., 1990) and the Kormann & Meixner (K&M) model (Kormann and Meixner, 2001), and a numerical Lagrangian Simulation (LS) model (Rannik et al., 2012). Details of the three models are described in the following subsections. The roughness changes caused by successive cuts of manipulated area during the course of the ME were taken into account for footprint modelling. For LS model, the roughness was directly included in the model inputs through the estimated parameter Z_0 (see details in the Section 2.3.3). In the analytical models used here, although the roughness length is not explicitly accounted for, the effect of changing roughness is indirectly included through the ratio U/u_* between mean horizontal wind speed U and friction velocity u_*, see Table 2. Model outputs with and without accounting for roughness variations have been compared to experimental footprint estimates α for each one of the three models in the ME. The two analytical models by Schuepp and K&M were compared to experimental footprint contributions only for neutral atmospheric stratification, while LS models runs have been executed in both neutral and unstable conditions. The two classes of stability were selected as follows: neutral for $-0.032 \leq (z-d)/L < 0.01$ and unstable for $-1 \leq (z-d)/L < -0.032$.

Table 2
Roughness length (Z_0) and ASL scaling coefficients of the wind speed components (a_u, a_v, a_w) estimated from vertical turbulence measurements at two heights in the ME case. The ratio U/u* estimated by a single point measurements is also reported.

	DOY: 132–139	DOY: 139–149	DOY: 149–155	DOY: 155–163
Z_0	0.118 m	0.082 m	0.057 m	0.037 m
U/u*	5.77	7.11	7.10	8.04
a_u	2.30	2.56	2.70	2.77
a_v	2.23	2.54	2.52	2.80
a_w	1.15	1.17	1.12	1.14

2.3.1. Schuepp analytical footprint model

The analytical Schuepp model estimates weighting factors of footprint function for scalar flux and concentration as analytical solutions of the advection-diffusion equation and has a simple formulation, which involves variables commonly measured at an EC site:

$$f(x) = \frac{(Uz_m)}{ku_*x^2} e^{\left(-\frac{Uz_m}{ku_*x}\right)} \quad (2)$$

where U is the mean horizontal wind speed, z_m is the measuring height and x is the horizontal upwind distance of the sources from the measurement system. This mathematical formulation allows an immediate and easy to use modelling of footprint function for each half-hourly period using variables (U, u_*) and parameters (z_m) measured on site. Another big advantage of this basic model is the negligible cost in terms of computational resources and complexities compared to more sophisticated and detailed models such as, e.g., Lagrangian Stochastic (LS) (Kljun et al., 2002; Kurbanmuradov and Sabelfeld, 2000) or Large Eddy Simulation (LES) models (Steinfeld et al., 2008). On the other hand the main limitations of this model are the poorly detailed quantification of processes concurring to the effective spatial distribution of scalar sources (turbulent wind field, surface roughness, topography, etc.), overestimation of source areas for both fluxes and concentrations and the validity restriction to near-neutral stability conditions (Schmid, 2002). Eq. (2) was used for the different values of the ratio U/u_* obtained in the different cuts, i.e. for similar roughness conditions of the cut plot. Input data for such variables were the averages of the ratio U/u_* calculated in each one of the four periods and during neutral atmospheric stability.

2.3.2. Kormann & Meixner analytical footprint model

The Kormann & Meixner (K&M) model is another analytical model but it is currently more often used for footprint analysis than the Schuepp model. Again it consists of an analytical function with variables measured by the EC system, but in this case parameters are

dependent on the atmospheric stability and this means that this model is more responsive to micrometeorological conditions than the Schuepp one. The K&M footprint function (Kormann and Meixner, 2001) is:

$$f(x) = \frac{1}{\Gamma(\mu)} \frac{\xi^{\mu}}{x^{1+\mu}} e^{\left(-\frac{\xi}{x}\right)} \quad (3)$$

where Γ is the Gamma function, μ is a parameter that depends on atmospheric stability conditions and ξ is a coordinate incorporating measurement height. The K&M model parameters were evaluated for each time averaging period using the tool available online at http://www.agroscope.admin.ch/art-footprint-tool/ (Neftel et al., 2008) with input variables calculated from measurements of wind speed and temperature. The values of parameters μ and ξ used for the K&M footprint model curves are the averages of the values of the same parameters obtained as output of the K&M footprint calculator. To reproduce the effect of roughness changes the K&M footprint model was also implemented separately for the four different cuts of the ME. For this reason values of the parameter μ and ξ were calculated for each extension of the Cut disc. Only periods of neutral atmospheric stability have been considered.

2.3.3. Lagrangian trajectory model and footprint calculation

A Lagrangian model for footprint calculation was applied releasing particles at the surface point source and tracking their trajectories downwind of this source towards the measurement location (Horst and Weil, 1992; Leclerc and Thurtell, 1990). The LS trajectory simulations were performed by using the three-dimensional model for inhomogeneous Gaussian turbulence by Thomson (Thomson, 1987). Particle trajectories and particle vertical velocities were sampled at the measurement height and the flux footprint function was estimated from these statistics. (Rannik et al., 2012). 10^6 trajectories were simulated. For AT experiment the commonly used cross-wind integrated footprint functions were estimated (Schmid, 2002). However, for the ME experiment, to account for the circular geometry of the source area border, integration of the footprint function was performed and presented over distance in radial coordinates. In LS simulations turbulence profiles were assumed to follow the atmospheric surface layer (ASL) regime. This was consistent with the limited simulation domain in horizontal direction up to 100 m only (in AT experiment). The profiles necessary for the LS dispersion model involved average horizontal wind speed, vertical momentum flux, variances of three wind speed components, dissipation rate of turbulent kinetic energy and vertical gradients of these statistics. The profiles were parameterized according to ASL similarity theory, including the stability dependence as presented by other authors (Högström, 1988; Kaimal and Finnigan, 1994). The measurements of turbulence statistics, namely three wind speed components and variances, momentum and sensible heat fluxes obtained at the measurement heights, were used in parameterization of turbulence profiles as follows:

- Roughness length z_0 was determined based on the momentum flux and wind speed measurements.
- The measured momentum and sensible heat fluxes were used to calculate the stability length L. However, in AT experiment neutral assumption was used due to small impact of stability considering low observation levels (0.7, 1.7 and 2.3 m).
- The variances of wind speed components (u, v and w denoting the along-wind, cross-wind and vertical speeds, respectively) and the friction velocity values were used to infer the proportionality coefficients $a_{u,v,w}$ for the ASL scaling profiles using the following relationship: $\frac{\sigma_{u,v,w}}{u_*} = a_{u,v,w} f(\frac{z}{L})$, where $f(\frac{z}{L})$ is the stability function (Kaimal and Finnigan, 1994).

The values obtained from measurements are reported in Tables 2 and 3, for the ME and AT case respectively. In the ME case the simultaneous measurement at two heights, 1.4 m and 2.35m, were used in estimation, whereas in AT the measurements at heights 0.7, 1.7 and 2.3 were used.

Table 3
Roughness length (Z_0) and ASL scaling coefficients of the wind speed components (a_u, a_v, a_w) estimated from vertical turbulence measurements at three heights in the AT case.

Z_0	0.018m
a_u	2.8
a_v	3.3
a_w	1.38

3. Results and discussion

3.1. Manipulation experiment

Experimental values of the flux contribution α from the vegetated surface in the ME (eq.1) decreased with the decreasing radius of the oats canopy with differences normally larger than experimental errors, starting from an initial value close to one. Values of α as a function of source area radius have been plotted with cumulative flux footprint as functions of distance obtained from the three different models in Figs. 4–6 . Both radius of the oat discs and the distance of the footprint function values were normalized by dividing them by the effective measurement height $h_{eff} = z_m - d$. LS cumulative footprint curves for each stability condition lie between that corresponding to the neutral case and that to the unstable case. The last one always predicts a smaller source area than the neutral one. This corresponds to theoretical expectation of sensing a reduced source area in unstable condition because the source area is restricted by enhanced convection and turbulent diffusion. However, for all three models a significant effect was played by accounting for roughness changes along the course of the manipulation, both directly by the roughness length parameter Z_0 in the LS models and indirectly by the ratio U/u_* in the analytical models. Estimates of Z_0, see section 2.3.3, decreased with reduction of the fetch and this is compatible with the reduced extension of dragging canopy. At the same time this was expected to affect the extension of the source area because lower roughness implies expansion of the footprint (Leclerc and Foken, 2014; Rannik et al., 2012). Table 2 resumes the average roughness changes and the evolution of wind profiles coefficients along the course of the ME as a consequence of the reducing fetch: the reduction of the roughness parameter estimated from two points profiles is quite evident, while the parameter a_w, that gives a quantification of the vertical turbulent diffusion, remains approximately constant and slightly lower than the commonly used value for ASL scaling, i.e. 1.25 (Foken, 2008). This means that, amongst the most important drivers of turbulent dispersion, roughness varied during the experiment significantly more than vertical velocity variance and for this reason it could be expected to have a significant effect on both the measurements and modelling of footprints. Analogously the values of the ratio U/u_* increased with the reducing sizes of the oats disc in the Managed plot, as a consequence of the reduced friction on the mean flow (see Table 2). In all cases the modelled footprint function values decrease when compared to the same model output without accounting for roughness change. Looking at the performances of the single models it appears qualitatively evident that LS models performs better than both analytical models. A quantitative estimate of the goodness of the agreement between models and experimental results in different conditions has been done using the root mean square error (RMSE) between the experimental footprint estimates and modelled cumulative footprint functions for the four upwind distances corresponding to the four radii of the Cut plot. In Table 4 the agreement is reported ranking

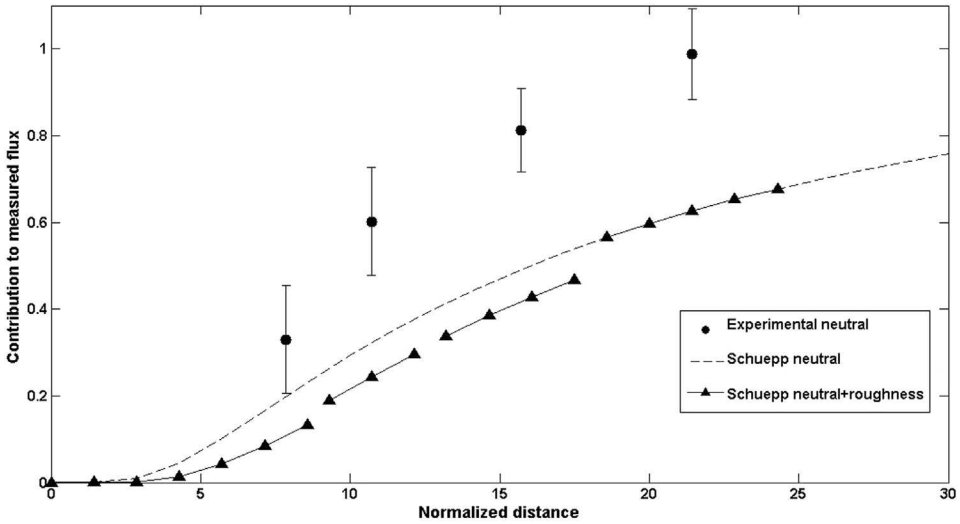

Fig. 4. Experimental flux contribution for different extensions of the managed plot in neutral conditions ($-0.032 <= (z_m - d)/L < 0.01$; dots) and Schuepp cumulative footprint for neutral conditions with (dashed lines with triangles) and without (dashed line) accounting for roughness change (for roughness values see Table 2). Roughness dependent Schuepp outputs have been plotted only for the space domain corresponding to its specific roughness. Distance was normalized dividing it by the effective measurement height $h_{eff} = z_m - d$.

the models by the increasing value of RMSE. The best agreement is reached by LS models when accounting for specific roughness conditions of the surface, followed by LS simulations without explicit roughness dependence. The improvement obtained by considering roughness is of the same order of magnitude but larger than that obtained running the LS in neutral instead of unstable conditions with the same roughness conditions. The discrepancy between models and experimental data increased for K&M and Schuepp models respectively, with both analytical models showing larger differences from experimental data when accounting for roughness conditions. For analytical models the variations due to the roughness has the same impact on the RMSE between models and data than for the LS models. Finally, the impact of the atmospheric stability on the experimental estimates of footprint has been evaluated computing the RMSE between experimental values of α estimated in neutral and unstable atmospheric stratifications. In this case the error was equal to 0.067, comparable with the variation in RMSE for LS models when accounting for specific roughness lengths. From these data it is possible to conclude that the surface roughness plays a role comparable and slightly larger in magnitude than that of atmospheric stability when modelling and measuring turbulent flux footprints. To assess the potential effect of IBL originated by the step roughness change, the ratio between u_* measured at two levels has been evaluated because a vertical variation of this variable is a direct result of IBL development (Garratt, 1992). A reasonable assumption is that the lowest measurement level of 1.4 m was always below the transition layer of the IBL, within the so-called Near Equilibrium Layer (NEL) where flow is in equilibrium with properties of underlying surface (Foken, 2008; Rao and Coté, 1974). In such conditions, an eventual IBL transition below the 2.35 m measurement level would have caused significant divergence and possible de-coupling between friction velocities at the two measurement levels. Variations in U/u_* ratio and effective roughness length estimates between the cut periods indicate that measurements were likely affected by IBL. Nevertheless a very high correlation has been found between u_* measurements at the two levels (for both whole experiment and single cut periods). The correlation coefficient for the full period was equal to 0.97 with slopes rather close to one for all periods (0.94 for entire experiment, ranging from 0.92 to 0.97 for the four cuts periods) indicating that turbulence characteristics were similar at both levels. This rather limited u_* divergence for an about

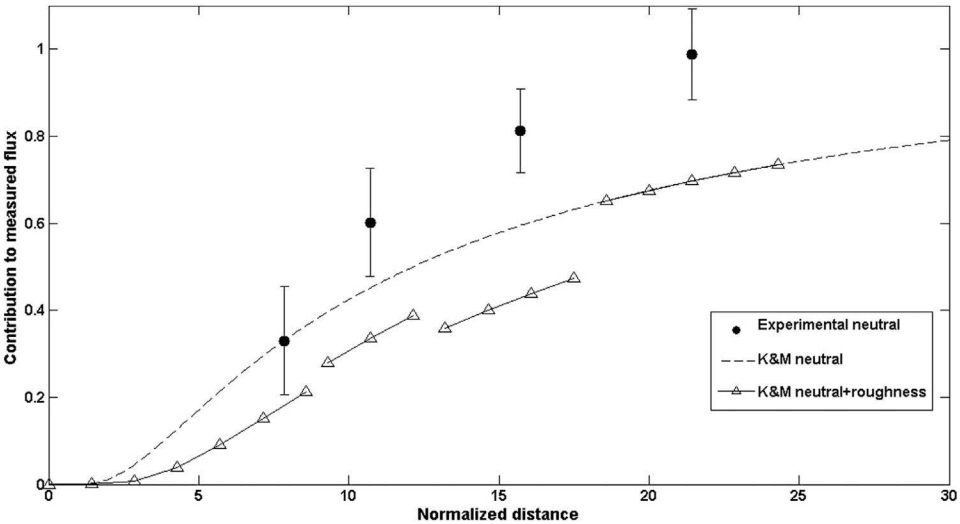

Fig. 5. Experimental flux contribution for different extensions of the managed plot in neutral conditions ($-0.032 <= (z_m - d)/L < 0.01$; dots) and K&M cumulative footprint for neutral conditions with (dashed lines with triangles) and without (dashed line) accounting for roughness change (for roughness values see Table 2). Roughness dependent K&M outputs have been plotted only for the space domain corresponding to its specific roughness. Distance was normalized dividing it by the effective measurement height $h_{eff} = z_m - d$.

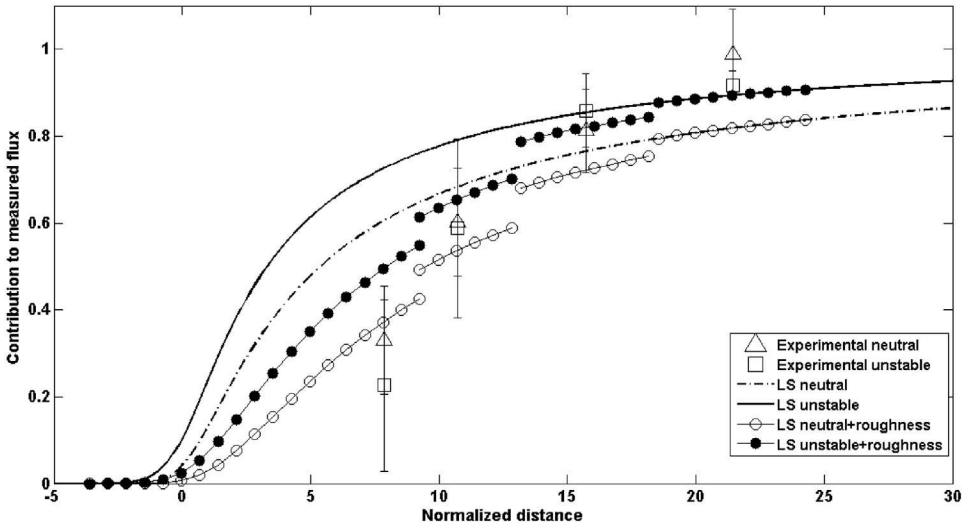

Fig. 6. Experimental flux contribution for different extensions of the managed plot in neutral ($-0.032 <= (z_m-d)/L < 0.01$; triangles) and unstable conditions ($-1 <= (z_m-d)/L < -0.032$; squares) and LS model cumulative footprint for neutral ($(z_m-d)/L = -0.005$) and unstable conditions ($(z_m-d)/L = -0.1$) with (lines with circles) and without (lines without circles) accounting for roughness change (for values see Table 2). Each couple of roughness dependent LS outputs, one for neutral (lines with empty circles) and one for unstable conditions (lines with filled circles), has been plotted only for the space domain corresponding to its specific roughness. Distance was normalized dividing it by the effective measurement height $h_{eff} = z_m - d$.

Table 4
RMSE between modelled and experimental footprint for the different cases of the ME. Models are ranked from the lowest to the highest error.

Model	RMSE
LS neutral + roughness	0.104
LS unstable + roughness	0.133
LS neutral	0.166
K&M neutral	0.197
LS unstable	0.217
K&M neutral + roughness	0.285
Schuepp neutral	0.287
Schuepp neutral + roughness	0.341

three-fold increase in effective measurement height suggests that the wind statistics within the IBL did not present severe deviations from undisturbed ASL relations. On the other hand, the variation of the effective roughness length evaluated through the ratio U/u_* reflected accommodation of average wind speed with distance to the roughness change and has been accounted for in models. This corresponds to the common practice for footprint modelling over heterogeneous surfaces when the applied models are developed for horizontally homogeneous conditions. Moreover the direct determination of roughness change effect would have required numerical experiments that were not part of this study. In conclusion the impact of IBL on the turbulence flow field can be expected to be rather limited and the footprint models accounted for it through the change in surface roughness, suggesting that both experimental estimates and models of footprint of this study were representing the specific field conditions in a reliable way.

3.2. Artificial tracer

Fig. 7 reports carbon fluxes measured during the AT experiment at three heights downwind and at one reference height upwind of the release line, normalized by the linear source emission strength of the artificial tracer release system. It can be observed that at a distance of approximately 40 m the contribution of released gas to the flux estimates becomes small at all three measurement heights (2.7 m, 1.7 m and 0.7 m), while there is a clear maximum contribution at shorter distances for all levels. The lower is the measurement height, the closer to the source this experimental footprint peak is. The shapes of experimental footprint curves, with a step growth for increasing distance toward a peak and a slower decrease beyond, are similar to what is expected from the theory and from the modelling results. The measurements obtained by the EC system upwind to the emission line are reported as a background reference to evaluate the measured flux in conditions presumably not affected by the released tracer. As expected in this reference case the measured fluxes at 2.3 m from the ground are negligible compared to the fluxes measured at all three heights downwind of the source and this background flux is almost zero for all positions of the release line. In Fig. 8 the experimental footprint values are plotted for each measurement level (0.7 m, 1.7 m and 2.3 m) against footprint functions modelled via K&M and LS footprint models. From this comparison the shape-similarity between experimentally derived and modelled footprints is more evident but also other quantitative conclusions can be highlighted. The experimentally derived footprint peak position is generally closer to the measurement point than the analytically modelled peak, especially at higher measurement heights while at the lowest measurement point the modelled footprint function is in better agreement with measurements. Instead Lagrangian simulations predict a footprint peak closer than experimental results for the lowest two measurement heights (0.7 m and 1.7 m), while it seems to be more in agreement at the higher level (2.3 m). Also in the latter case the overall shape of the footprint function is quite similar to the trend of experimental data whose magnitude remains significantly higher than the modelled one. This could be due to the fact that emitted flux is diluted more by crosswind and alongwind dispersion during the transport towards higher measurement systems, especially at longer distances, resulting in relatively lower flux detected by the higher EC measurement systems. Another important observation is that a small, but noticeable contribution of downwind emissions, i.e. when distance of the release line is negative, is detected by the highest measurement system while the lowest ones do not seem to be affected. This small contribution is not predicted by analytical models used in this study and the LS model reports non-negligible downwind contribution only for the highest measurement level. The fact that it is not revealed by the lowest measurement systems can be due to the length scale of the turbulent transport mechanism responsible for the backward diffusion that is too long to be detected by the lowest EC systems. The function describing the K&M footprint, i.e. Eq. (3), has been also fitted to the experimental dataset excluding the negative x-values corresponding to the downwind position of the

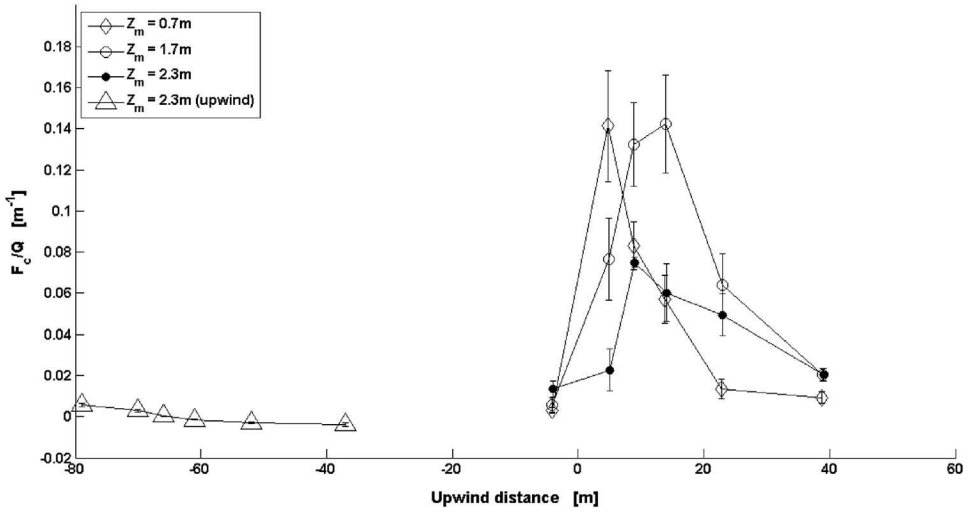

Fig. 7. CO_2 fluxes (Fc) measured by EC systems at three measurement heights and by the upwind reference EC system as a function of downwind distance of the emission line. Fluxes are normalized dividing by the linear source emission strength (Q).

release line because the function is not defined in such a domain. For each level the upwind location of the footprint function peak, that represents the distance of the sources mostly contributing to the measured flux, and the upwind distance at which the cumulative footprint reaches a fraction of the total flux, respectively 50%, 75% and 90%, for the fitted K&M model are reported in Table 5. In Table 6 the same parameters are reported for Lagrangian simulations. The close proximity to the measurement systems of both the footprint peak and the upwind contribution to the flux (e.g. 75%) are remarkable experimental evidences that fetch requirement on EC measurements was generally overestimated in the past using rules of thumbs, assuming source areas extended up to 100 times the measurement height or more. Roughly speaking 75% of the flux derives from an area bound by an upwind distance that is between 20 and 30 times the effective measurement height (h_{eff}) or down to 15*h_{eff} if we consider more advanced numerical Lagrangian simulation, while the highest contribution comes from an upwind distance that is 4.9*h_{eff} to 7.1*h_{eff} or, surprisingly close, only between 2.6*h_{eff} and 4.2*h_{eff} according to Lagrangian simulations. In AT experiment the values $a_{u,v,w}$ used for LS simulations differ from the averages usually obtained for steady ASL conditions, respectively 2.45, 1.9 and 1.25 (Foken, 2008), see Table 3. The difference is largest for the vertical a_w and the cross-wind component a_v. Significantly higher value for a_v probably reflects the sporadic nature of turbulence prevailing during the observation conditions, but trajectory dispersion in alongwind direction is not affected by this value, implying that the cross-wind integrated footprint function does not depend on it. However, the vertical dispersion is sensitive to the variance of the vertical wind speed and higher value of a_w results in enhanced vertical dispersion. For this reason footprints obtained by LS

Table 5
Parameters of the K&M footprint function outputs fitted to experimental data at each measurement level, divided by the corresponding measurement heights: (X_peak/Z_m) is the position of the footprint curve peak, (X(50%)/Z_m; X(75%)/Z_m and X(90%)/Z_m) are upwind distances of the sources contributing up to 50%, 75% and 90%, respectively, of the measured flux.

Z_m	X_peak/Z_m	X(50%)/Z_m	X(75%)/Z_m	X(90%)/Z_m
2.3 m	4.87	10.96	21.7	42.93
1.7 m	6.47	11.12	18.77	32.42
0.7 m	7.14	15.00	28.87	58.16

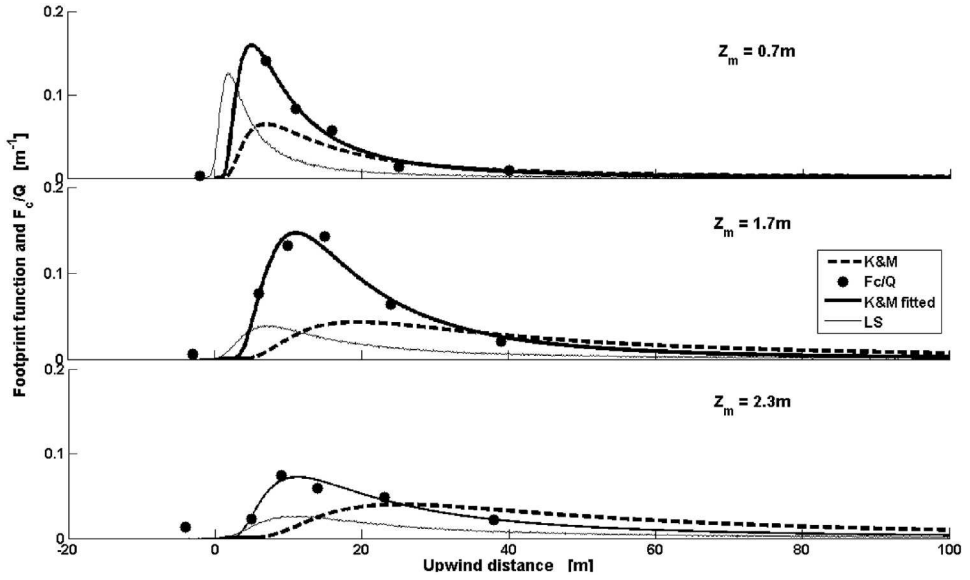

Fig. 8. CO_2 fluxes (Fc) divided by linear source emission strength (Q) (filled circles), K&M footprint curve (dashed line), K&M adapted footprint curve from fitting to experimental data (continuous thick line) and LS footprint curve (continuous thin line). Panels from the top correspond respectively to measurement heights 0.7m, 1.7 m and 2.3 m.

Table 6
Parameters of the LS footprint function outputs obtained from simulated curves for each measurement level, divided by the corresponding measurement heights: (X_{peak}/Z_m) is the position of the footprint curve peak, ($X(50\%)/Z_m$; $X(75\%)/Z_m$ and $X(90\%)/Z_m$) are upwind distances of the sources contributing up to 50%, 75% and 90%, respectively, of the measured flux.

Z_m	X_{peak}/Z_m	$X(50\%)/Z_m$	$X(75\%)/Z_m$	$X(90\%)/Z_m$
2.3 m	4.17	8.35	15.17	24.13
1.7 m	4.21	9.5	18.5	32.62
0.7 m	2.64	7.21	16.5	37.79

method are contracted in the along-wind direction, resulting in closer positioning of the footprint peaks. Finally, a sensitivity test with respect to the limited length of the emission line was performed by LS modelling because crosswind dispersion could be responsible for further uncertainty in the measurements and modelling of footprint functions, in particular if impacting differently the results for three measurement levels. LS simulations were done assuming 40 m and infinite release line lengths for the three measurement heights. This sensitivity analysis can only provide a theoretical estimation of this effect, based on the ability of used LS models to reproduce crosswind dispersion and hence to provide an approximation for an effect that was not possible to evaluate experimentally for logistic reasons. However, the results of such different model runs were almost identical (data not shown) at all distances and for all measurement heights, suggesting that the assumption of negligible impact of the limited line source and crosswind dispersion is reliable. Possible bias due to the wind direction was also excluded because the wind directions measured during the experiment varied by less than ± 15° around the mean values.

4. Conclusions

Two experimental studies of the source area for EC fluxes have been realized above a grassland to provide in situ data for experimental validation of footprint models. The first set-up consisted in a manipulation (ME) of the area surrounding the EC tower with successive concentric cuts to quantify the effects of its changing extension on the measured flux, compared to an uncut surface. In the second test an artificial linear tracer emission system was implemented (AT) to test the response induced on EC measurements at different heights by placing sources at variable distances from the sensors, both upwind and downwind. In both cases experimental footprint estimates have been compared with models of increasing complexity and accuracy to provide a field validation because there is a significant lack of data in current literature and experimental realization of this kind are extremely rare, especially like the ME. The measurements are in good agreement with footprint models used, in particular with regard to the shape of the footprint curve and the order of magnitude of source area extension. Another major outcome of this study is the significant impact of the roughness and turbulence field characterization on the footprint estimates. Particularly in the case of the LS models and the ME experiment, providing a more detailed characterization of the roughness parameter and turbulence statistics has substantially improved the agreement between experimental data and numerical simulations. This improvement has been quantitatively more effective than taking into account the effect of atmospheric stability when using LS models, at least for the stability conditions presented here and for the surface of this specific case. These results suggest that detailed description of the roughness and vertical turbulence structure, can lead to significant improvement in footprint prediction in complex cases such as e.g. in heterogeneous source areas, small fetches and complex topography. In this context the use of emerging remote and proximal sensing technologies as LIDAR for canopy structure description and vertical wind profiling can be extremely useful. Quantitative results of modelled and measured footprints are obviously site- and setup-specific, but their relation to measurement heights serve as a useful tool for practical evaluation of source area extension. Resuming the results in both experiments, except for measurements carried out exceptionally close to the ground, sources for the major fraction of the measured fluxes, i.e. more than 75% of flux contributions, are confined within a range of upwind distances between ten or twenty times the effective measurement height. This is the height respect to zero-plane displacement and not to the soil. To give an idea an EC system placed at 3.5 m above the soil in a 2 m high dense crop has most of its flux source area limited from 20 to 40 m upwind. Accordingly, the peak of the flux contribution was confined to approximately five times the effective measurement height. The good qualitative accordance of LS models with experimental data partly confirms the findings of the few available experimental footprint studies (Göckede et al., 2005; Leclerc et al., 2003). Also, the order of magnitude of source area extension and footprint peak position can be compared to other findings, while the effect of atmospheric stability on experimental estimates was smaller than in other studies, e.g. (Marcolla and Cescatti, 2005) but in the present study stable stratifications have not been considered. Further validation experiments of this kind are necessary for the improvement of footprint modelling but detailed descriptions of turbulence and aerodynamic properties of micrometeorological sites are also extremely important and can be used to provide more detailed footprint modelling without adding complex and expensive measurements to the existing infrastructures.

Acknowledgements

Authors are extremely grateful to Raffaele Casa, Fabio Pieruccetti and Sergio Pampaloni for their unvaluable and fundamental support in the implementation of the two experimental setup's in the terrains of the Azienda Agraria Didattico-Sperimentale "Nello Lupori" of University of Tuscia. Sincere acknowledgements also for Carlo Trotta, Alessio Ribeca and Oscar Perez-Priego for their help in field logistic, as well to Sami Haapanala for providing some of the instruments used during the experiment. Authors have found extremely helpful most of the comments by anonymous reviewers because they have strongly pushed and driven the manuscript improvement and for this reasons they deserve a special gratitude. A special thanks to Josie Meaney for her sincerely appreciated proofreading of the manuscript.

NA thanks the support from ICOS-Belgium and Fonds Wetenschappelijk Onderzoek (FWO)

AC thanks the support from projects DESESTRES (PROMETEOII/2014/038) and GEISpain (CGL2014-52838-C2-2-R).

DP thanks the support from the ENVRIPLUS project funded by the European Union's Horizon 2020 research and innovation programme under grant agreement No. 654182.

TV thanks the support from the Academy of Finland Centre of Excellence (118780), Academy Professor projects (1284701 and 1282842) and ICOS-Finland (281255)

References

Aubinet, M., et al., 1999. Estimates of the annual net carbon and water exchange of forests: the EUROFLUX methodology. In: Fitter, A.H., Raffaelli, D.G. (Eds.), Advances in Ecological Research. Academic Press, pp. 113–175.
Aubinet, M., et al., 2001. Long term carbon dioxide exchange above a mixed forest in the Belgian Ardennes. Agric. Forest Meteorol. 108 (4), 293–315.
Finn, D., Lamb, B., Leclerc, M.Y., Horst, T.W., 1996. Experimental evaluation of analytical and Lagrangian surface-layer flux footprint models. Bound. Layer Meteorol. 80 (3), 283–308.
Foken, T., Leclerc, M.Y., 2004. Methods and limitations in validation of footprint models. Agric. Forest Meteorol. 127 (3–4), 223–234.
Foken, T., 2008. Micrometeorology. Springer-Verlag, Berlin, Heidelberg.
Göckede, M., Rebmann, C., Foken, T., 2004. A combination of quality assessment tools for eddy covariance measurements with footprint modelling for the characterisation of complex sites. Agric. For. Meteorol. 127 (3–4), 175–188.
Göckede, M., et al., 2005. Validation of footprint models using natural tracer measurements from a field experiment. Agric. For. Meteorol. 135 (1–4), 314–325.

Garratt, J.R., 1992. The Atmospheric Boundary Layer Cambridge Atmospheric and Space Science Series. Cambridge University Press.
Högström, U.L.F., 1988. Non-Dimensional wind and temperature profiles in the atmospheric surface layer: a Re-Evaluation. In: Hicks, B.B. (Ed.), Topics in Micrometeorology. A Festschrift for Arch Dyer. Springer, Netherlands, Dordrecht, pp. 55–78.
Horst, T.W., Lenschow, D.H., 2009. Attenuation of scalar fluxes measured with spatially-displaced sensors. Bound. Layer Meteorol. 130 (2), 275–300.
Horst, T.W., Weil, J.C., 1992. Footprint estimation for scalar flux measurements in the atmospheric surface layer. Bound. Layer Meteorol. 59 (3), 279–296.
Kaimal, J.C., Finnigan, J.J., 1994. Atmospheric Boundary Layer Flows: Their Structure and Measurement. University Press, Oxford.
Kljun, N., Rotach, M.W., Schmid, H.P., 2002. A three-dimensional backward Lagrangian footprint model for a wide range of boundary-layer stratifications. Bound. Layer Meteorol. 103 (2), 205–226.
Kormann, R., Meixner, F.X., 2001. An analytical footprint model for non-neutral stratification. Bound. Layer Meteorol. 99 (2), 207–224.
Kristensen, L., Mann, J., Oncley, S.P., Wyngaard, J.C., 1997. How close is close enough when measuring scalar fluxes with displaced sensors? J. Atmos. Oceanic Technol. 14 (4), 814–821.
Kurbanmuradov, O., Sabelfeld, K., 2000. Lagrangian stochastic models for turbulent dispersion In the atmospheric boundary layer. Bound. Layer Meteorol. 97 (2), 191–218.
Leclerc, M.Y., Foken, T., 2014. Footprints in Micrometeorology and Ecology. Springer-Verlag, Berlin Heidelberg.
Leclerc, M.Y., Thurtell, G.W., 1990. Footprint prediction of scalar fluxes using a Markovian analysis. Bound. Layer Meteorol. 52 (3), 247–258.
Leclerc, M.Y., Meskhidze, N., Finn, D., 2003. Comparison between measured tracer fluxes and footprint model predictions over a homogeneous canopy of intermediate roughness. Agric. For. Meteorol. 117 (3–4), 145–158.
Marcolla, B., Cescatti, A., 2005. Experimental analysis of flux footprint for varying stability conditions in an alpine meadow. Agric. For. Meteorol. 135 (1–4), 291–301.
Moncrieff, J.B., et al., 1997. HAPEX-SahelA system to measure surface fluxes of momentum, sensible heat, water vapour and carbon dioxide. J. Hydrol. 188, 589–611.
Neftel, A., Spirig, C., Ammann, C., 2008. Application and test of a simple tool for operational footprint evaluations. Environ. Pollut. 152 (3), 644–652.
Nicolini, G., et al., 2015. Performance of eddy-covariance measurements in fetch-limited applications. Theor. Appl. Climatol. 1–12.
Rannik, Ü., et al., 2012. Footprint analysis. In: Aubinet, M., Vesala, T., Papale, D. (Eds.), Eddy Covariance A Practical Guide to Measurement and Data Analysis. Springer Atmospheric Sciences, Springer; Netherlands.
Rao, K.S.W., Coté, J.C., 1974. The structure of the two-dimensional internal boundary layer over a sudden change of surface roughness. J. Atmos. Sci. 31, 738–746.
Rebmann, C., et al., 2005. Quality analysis applied on eddy covariance measurements at complex forest sites using footprint modelling. Theor. Appl. Climatol. 80 (2), 121–141.
Rebmann, C., et al., 2012. Data acquisition and flux calculations. In: Aubinet, M., Vesala, T., Papale, D. (Eds.), Eddy Covariance A Practical Guide to Measurement and Data Analysis. Springer Atmospheric Sciences, Springer, Netherlands.
Reichstein, M., et al., 2005. On the separation of net ecosystem exchange into assimilation and ecosystem respiration: review and improved algorithm. Glob. Change Biol. 11 (9), 16.
Schmid, H.P., 1994. Source areas for scalars and scalar fluxes. Bound. Layer Meteorol. 67 (3), 293–318.
Schmid, H.P., 2002. Footprint modeling for vegetation atmosphere exchange studies: a review and perspective. Agric. For. Meteorol. 113 (1–4), 159–183.
Schuepp, P.H., Leclerc, M.Y., MacPherson, J.I., Desjardins, R.L., 1990. Footprint prediction of scalar fluxes from analytical solutions of the diffusion equation. Bound. Layer Meteorol. 50 (1), 355–373.
Steinfeld, G., Raasch, S., Markkanen, T., 2008. Footprints in homogeneously and heterogeneously driven boundary layers derived from a lagrangian stochastic particle model embedded into large-Eddy simulation. Bound. Layer Meteorol. 129 (2), 225–248.
Thomson, D.J., 1987. Criteria for the selection of stochastic models of particle trajectories in turbulent flows. J. Fluid Mech. 180, 28.
Vesala, T., et al., 2008. Flux and concentration footprint modelling: state of the art. Environ. Pollut. 152 (3), 653–666.
Webb, E.K., Pearman, G.I., Leuning, R., 1980. Correction of flux measurements for density effects due to heat and water vapour transfer. Q. J. R. Meteorolog. Soc. 106 (447), 16.